DOI: 10.13009/EUCASS2023-092
Aerospace Europe Conference 2023 – 10TH EUCASS – 9TH CEAS

Unsteady Vortex Lattice Method in Tornado: A Fast and Cost-Effective Solver for Dynamic Analysis of Supersonic Lifting Surfaces

Hemant Joshi[⋆†] *and Peter Thomas*[⋆]
[⋆]*Centre for Engineering Research, University of Hertfordshire*
College Lane Campus, Hatfield, Hertfordshire, UK
h.joshi2@herts.ac.uk · p.thomas5@herts.ac.uk
[†]Corresponding author

Abstract
This study details the development of the Unsteady Vortex Lattice Method (VLM) in conjunction with the MATLAB based Tornado VLM software, aiming to enhance the capabilities of Tornado for unsteady analysis. This integration allows for improved accuracy and computational efficiency in predicting the dynamic behaviour of such surfaces. The following work is based on the frequency response of the generalised VLM that effectively removes the cost associated with higher-order computational fluid dynamics (CFD) solvers. The solver works on the framework of adaptive time-step response and reduces the truncation error improving the accuracy. This unsteady solver computes the induced flow to calculate the forces acting on the panel concerning time. This unsteady VLM is a fast mode of solver for predicting the dynamic behaviour of a lifting surface which enables its use in quicker preliminary design analysis. The results were compared with conventional CFD simulation and have seen a comparable accuracy for reduced run time. Being a lower-order method, the solver is 24 times faster than the CFD simulation, which reduces the cost associated and computational power requirement.

Nomenclature

α	Angle of Attack
α_x	Angle of attack position in x
α_y	Angle of attack position in y
β	Side-slip angle
Γ	Bound Circulation of an aerofoil
ω	Frequency of oscillation
$C_{L\alpha}$	Lift curve slope with α
u	Free stream Velocity
C_D	Coefficient of Drag
C_L	Coefficient of Lift
dt	Time step response
LOM	Low-order Modelling
MAC	Mean aerodynamic chord
URANS	Unsteady Reynolds Average Navier Stokes
UVLM	Unsteady VLM
VLM	Vortex Lattice Method

DOI: 10.13009/EUCASS2023-092

1. Introduction

Fluid dynamics is a sub-discipline of fluid mechanics that encompasses aerodynamics and hydrodynamics. These fields are important for engineering design and analysis. Unsteady aerodynamics has been studied for over a century to better understand the flow around aircraft undergoing unstable dynamic motion due to gusts, side-slip or rapid manoeuvring. This analysis is critical for designing aerofoils and other aerodynamic implements. The theory of unsteady aerodynamics began in early 1920 with Theodorsen's approach[26] for analysing oscillating aerofoils. The Wagner function[28] was then used to study the separated flow in an unsteady manoeuvre, while the Kussner function[10] resolved the issue of the shed vortex's gradual reduction in influence on the aerofoil over time. The VLM, which emerged in 1937,[19] revolutionized the analysis of the aerodynamic sections of wings by dividing them into panels, providing a sectional overview that was widely used in early aircraft design. VLM can also be used to solve unsteady aerodynamics based on the unsteady lifting line theory[22] for dynamic motion that changes over time. Unsteady aerodynamics is complex to model and requires significant computational power and time to analyze. To improve the efficiency of computational simulations for unsteady modelling, low-order methods like VLM have proven to be effective[24] . Low-order modelling (LOM) is an increasingly popular approach that utilizes classical potential and lifting line theory to create new design tools focusing on reduced parameters. This approach is essential for early design work, as it reduces the number of parameters, complex calculations, and the time required[5] .

The fundamental use of low-order solvers is to reduce the number of degrees of freedom required to produce the results for the required performance. VLM or panel methods are effective low-order approaches in calculating the pressure change with the help of velocity change over a wing divided into several panels.[12] The change in velocity is calculated with induced vortices generated over each panel. Each panel is associated with its control point (collocation point) from which the velocity potential is computed. The resultant velocity, with relation to the free-stream velocity and Kutta's condition[4] provides the solution of the vortex strength, and through the integration of those, lift and induced drag forces are calculated. The output of this method can predict the stability derivatives and aerodynamic characteristics of flying objects. A key difference between a steady solver and unsteady VLM (UVLM) is the need to use time steps whereby each vortex's calculation over a panel is obtained at each time step as shown in Fig. 1. The use of LOM has been in place for more than a decade with its first-ever unsteady implementation in the 1990s[5] . These methods are computationally efficient enough to predict the unsteady aerodynamic loads[31] . They are ways of solving for three-dimensional flow fluids like pressure and velocity when compared with conventional CFD-based interpolation methods. Initially, the LOM approach is divided into two subroutines: time-based response and frequency-based response. With the time-based response, every parameter starting from flow speed, location of the aerofoil and many others will be changed with respect to time to model the dynamic nature of the flow around a vibrating or heaving aerofoil. With the frequency-based response, these changes are more dominated by frequency change than time. This approach was used in the aeroelastic analysis of active control for flutter and gust response[14] . Because of this effectiveness, LOM

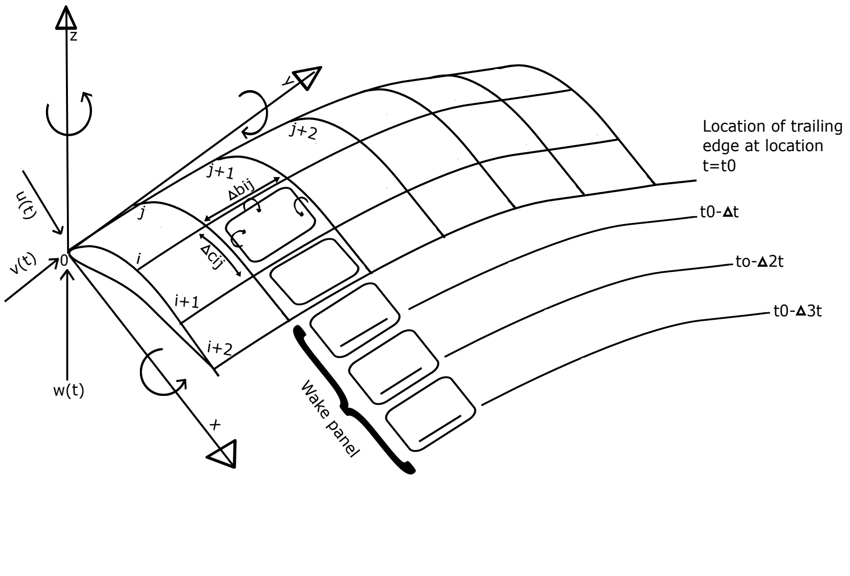

Figure 1: Unsteady vortex lattice representation[3]

DOI: 10.13009/EUCASS2023-092

approaches are widely used in the early design process stages to speed up the unsteady analysis.

Tornado is a MATLAB-based implementation of VLM[16] that is being used as a framework to develop and implement LOM using UVLM. The UVLM equations are defined in matrices for easy and quick calculations. The solver allows the user to define the heaving motion with two parameters i.e., heaving amplitude which is the function of the base chord of an aerofoil, and heaving frequency which is the function of true airspeed. The location of the most recently shed wake is calculated from the initial time-step response. The subroutine solves for two-dimensional aerodynamic analysis of an aerofoil of a stated wing of a designed aircraft under given flow conditions. The proposed program is a quick unsteady solver which differs from conventional CFD modelling with respect to solver time and analysis. The use of such LOM methods is beneficial for the preliminary design of the next generation of aircraft. The developed solver can predict the lift, drag and moment coefficients in seconds which drastically cuts computational costs. Since it is based on the LOM approach, the solver can run on less powerful computer systems as compared to the ones used for CFD simulations. Cost is one of the major reasons for design problems in the next generation of aircraft designs, this solver holds good potential for implementation in early design optimisation work. In this paper, the results of the 2D UVLM code are presented and compared against a higher-order CFD simulation after its validation with experimental and analytical results.

2. Theoretical Approach: Unsteady vortex lattice method

When visualizing certain flights the inclusion of wake analysis is always helpful in tracking the motion of an aircraft. Studies have shown that Theodorsen's theory[26] is remarkable in predicting unsteady aerodynamics of the lifting surface and still holds the same for high-intensity sinusoidal motions. Predicting the non-periodic motion is done by super-imposing Wagner's function[28] . Besides these classical theories, UVLM can be used for lower-order modelling. This method is extended to implement the 2D unsteady wake from the trailing edge. The boundary conditions and influence matrix from wake and bound vortices have been re-derived with respect to time which changes for every time step response. The lift coefficient is derived from the rate of change of bound circulation with respect to time[25] . The field of unsteady aerodynamics completely depends on past motion, i.e., the history associated with the motion with respect to time, and the repetition of that motion which means how often it repeats (which is dependent on frequency). It has been seen from all the unsteady theories of the past[11] ,[2] ,[21] ,[17] that every flow field is time dependent which depends on its state, velocity and temperature of the flow. The major difference between unsteady and steady VLM is the inclusion of wake modelling to account for the 3D interference during unsteady flow conditions. The transition of conventional VLM to UVLM is mainly driven by viscous phenomena, such as the need to study the leading-edge separation for delta wings. The UVLM helps in calculating the velocity potential with the help of boundary conditions which is the basis of the unsteady potential flow theory[7] .

2.1 Oscillating aerofoils

Oscillating aerofoils under the influence of unsteady motion such as heaving, pitching and the combination of both, have been used to examine high forward thrust and help in analysing unsteady aerodynamics[29] . Such complex modelling is highly effective in analysing the flapping wings of insect or bird flight, MAV (Micro air vehicle), UAV (unmanned air vehicle), and VTOL (Vertical take-off and landing) flights[9] . The use of this modelling is also seen with aeroelastic analysis of wind turbines under heavy crosswinds. The motion of an aerofoil which is time dependent is essential in visualising vorticity contours around an aerofoil oscillating with heaving amplitude. The vorticity fields are initially generated at low speeds and are governed by time instances. The heaving motion of an aerofoil shown in Fig. 3 is governed by its frequency and amplitude[13] which in this case is the function of the base chord and velocity of flow. The heaving motion also helps in understanding the vortex shedding[27] , which is seen after a single time step. The generated vortices will shed off from the trailing edge which, when separated over time, forms the bound vortex which creates the high-pressure region under the aerofoil essentially increasing the lift generation. Pitching motion leads to changes in the orientation of an aerofoil for a varying range of angle of attack in each time frame as shown in Fig. 2 and 3. The body axis of an aerofoil is fixed at MAC (Mean aerodynamic chord) to provide a reference system around which the body axis will change. A pitching aerofoil helps in visualising both leading edge and trailing edge vortex shedding[23] . The recent investigation of this motion is done with different aerofoil arrangements[30] for visualising the flow separation over pitching and plunging aerofoils. That research proves the viability of accurately predicting a surging and pitching wing vortex formation. It shows that the accuracy holds good for potentially low order models[9] and justifies its use with reduced order modelling. The paper by Moriche *et al.*[18] shows the use of this approach for predicting the leading edge suction parameter, which states that the given aerofoil before experiencing any flow separation with respect to time can suffer a finite amount of flow suction which is very essential information in predicting vortex formation.

DOI: 10.13009/EUCASS2023-092

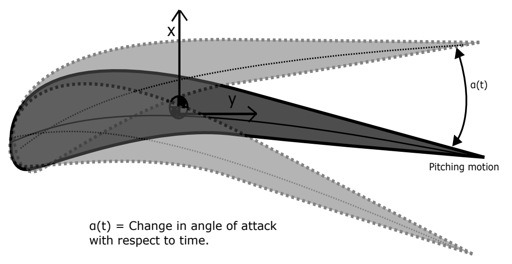

Figure 2: Pitching aerofoil with time-step.

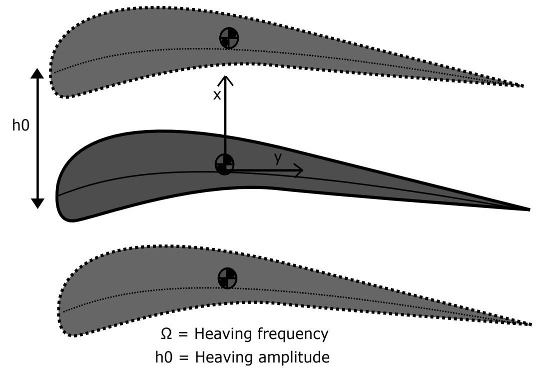

Figure 3: Heaving aerofoil with time-step.

2.2 Boundary conditions for an oscillating aerofoil

The coordinate system for a heaving aerofoil is derived with respect to time as shown in Fig. 4. As the heaving motion is based on heaving frequency and amplitude, the location of the aerofoil moving up and down only has an effect on the y-axis position, whereas the x-axis is the function of flow speed and time. At each discrete time step, the location of shed vortices from the trailing edge is re-calculated to trace its path. As time $t > 0$ the aerofoil starts moving up following the time-dependent path.

$$s_x = -v \times t \qquad (\text{x} - \text{coordinate}) \tag{1}$$

$$s_y = -h_0 \times \sin(\omega \times t) \qquad (\text{y} - \text{coordinate}) \tag{2}$$

The unsteady motion of an aerofoil under flow with reference to the body frame is given by:

$$(\Delta\phi - V - \omega \times r) \cdot n = 0 \tag{3}$$

where V is the flow velocity, $\Delta\phi$ is the change of velocity potential, ω is the frequency of rate of change of body axis with respect to time, r is the position vector from body axis to most recently shed wake and n is the normal vector. The trailing vortex location is given by:

$$x = (C + dx) \times \cos(\alpha) + s_x \tag{4}$$

$$y = -(C + dx) \times \sin(\alpha) + s_y \tag{5}$$

where c is the base chord, dx is the location of most recently shed vortices with respect to time, α is the angle of attack and s_x, s_y are the body coordinates with respect to time t. The location of the bound vortices with respect to t is given

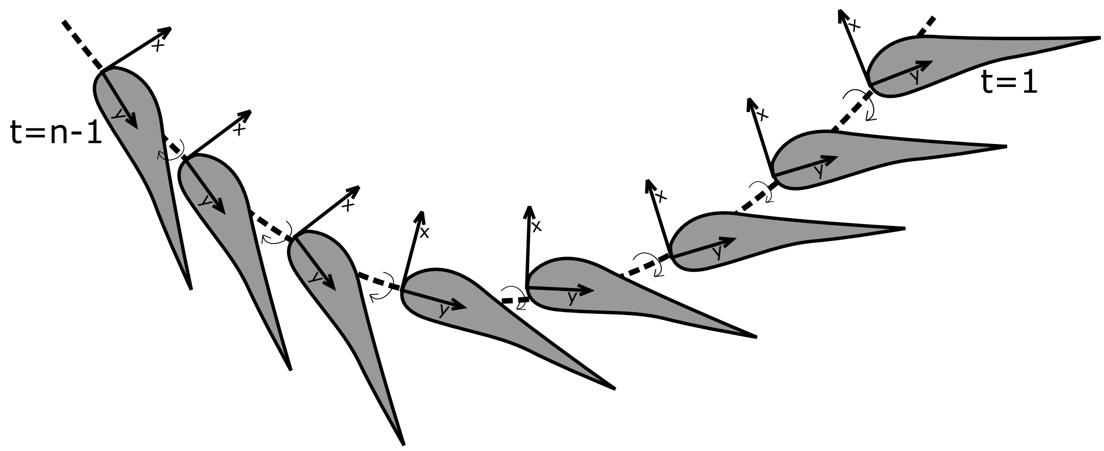

Figure 4: Aerofoil location with time step

DOI: 10.13009/EUCASS2023-092

by:

$$x_1 = \frac{1}{4} \times C \times \cos\alpha + s_x \tag{6}$$

$$y_1 = \frac{1}{4} \times C \times \sin\alpha + s_y \tag{7}$$

Calculation of wake downwash using Biot-Savart Law is given by:

$$W = u \times \sin\alpha + w \times \cos\alpha \tag{8}$$

Here W is the wake-induced downwash, while u and w are the sum of all induced velocities from the wake elements of interest. The lift and drag on an aerofoil are because of only normal forces and rate of bound circulation with respect to time which is given by:

$$\overline{q} = \frac{1}{2} \times \rho \times (V + w(it))^2 \tag{9}$$

$$C_l = \frac{L(it)}{\overline{q(it)} \times C} \tag{10}$$

$$C_d = \frac{D(it)}{\overline{q(it)} \times C} \tag{11}$$

Here $\overline{q}$ is the kinetic (or dynamic) pressure, $w(it)$ is induced velocity for a single iteration, ρ is the density of air at sea level, $L(it)$ is the calculated lift for a single iteration, $D(it)$ calculated drag (induced drag) for a single iteration. It can be seen that the given unsteady boundary conditions follow Theodorsen's approach as the position of the geometry is a function of time and frequency of the motion shown in equations 1 and 2. Since the unsteady motion of a flow under an aerofoil is defined as the change in frequency of the motion multiplied by the position vector r and the normal vector n. The change in velocity potential is calculated over each change in this position shown in equation 3.

3. Computational Approach: Implementation with Tornado

An aircraft wing is defined in Tornado from the information provided by the user. The wing geometry and flight state conditions are provided by the user, from which the program works out the ISA conditions for the density of air and

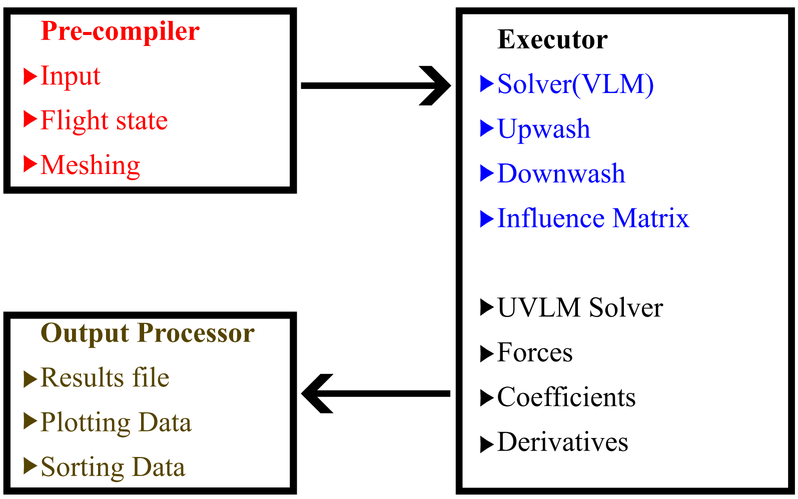

Figure 5: Tornado layout with UVLM.

DOI: 10.13009/EUCASS2023-092

other relevant information. After the completion of initialisation, the program moves to the solver which gives the user the option to select the mesh type and solver type according to his requirements. After that, the results are saved for future analysis and graphs are plotted for visual and data analysis as shown in Fig. 5 This solver holds good potential for quickly analysing the aerodynamics for a defined geometry under given conditions.[3] To model the dynamic motion of an aerofoil, a new section of the processor is written to implement the 2D UVLM. The code works in predicting the heaving and pitching motion of an aerofoil based on the frequency and amplitude of the wave. The defined motion is a function of the uniform velocity and the base chord. The time step is implemented within the UVLM solver to provide the change in aerodynamic characteristics of an aerofoil with respect to time.[20] With using this solver with co-relation to Tornado the initialisation parameter required for this solver is extracted from the Tornado base code and directories. The representation of this, as integrated into the existing Tornado code, is shown in Figure 6. The results obtained are stored in the same results file with a different name to simplify visualization and distinguish between the steady and unsteady results. In Fig. 6 the blue colour highlighted area is part of the main section of Tornado code, which works around by asking questions to the user for the initial geometry set-up, flight state model and lattice setup which is colour coded in red. The solver predicts the aerodynamic characteristics for analysis over defined geometry using initial conditions and calculates forces acting on panels which is colour coded in brown colour. These results files are then used by force coefficients subroutines which are colour coded in dark green colour. This representation is the basic layout of the Tornado framework subroutines which work in conjunction to predict the steady state response of user-defined motion. In addition to these two new cases are added to improve Tornado's unsteady application capability for oscillatory aircraft analysis. In Fig. 6 the top left corner has two solver's subroutines named UVLM (Unsteady VLM for two-dimensional analysis) and UVLM-3D (Unsteady VLM for three-dimensional wing profiles). UVLM has subsections code which defines the oscillatory motions of an aerofoil with heaving or pitching motion based on the frequency and time step response as the function of chord length. An adaptive time-step response has been added to these subroutines to added it to improve the computational speed whilst retaining good accuracy by defining the parameter called truncation error which is the difference in predicted values from real values. The code workout to change the time-step to accommodate that change for improved accuracy of the results. The calculated results files are

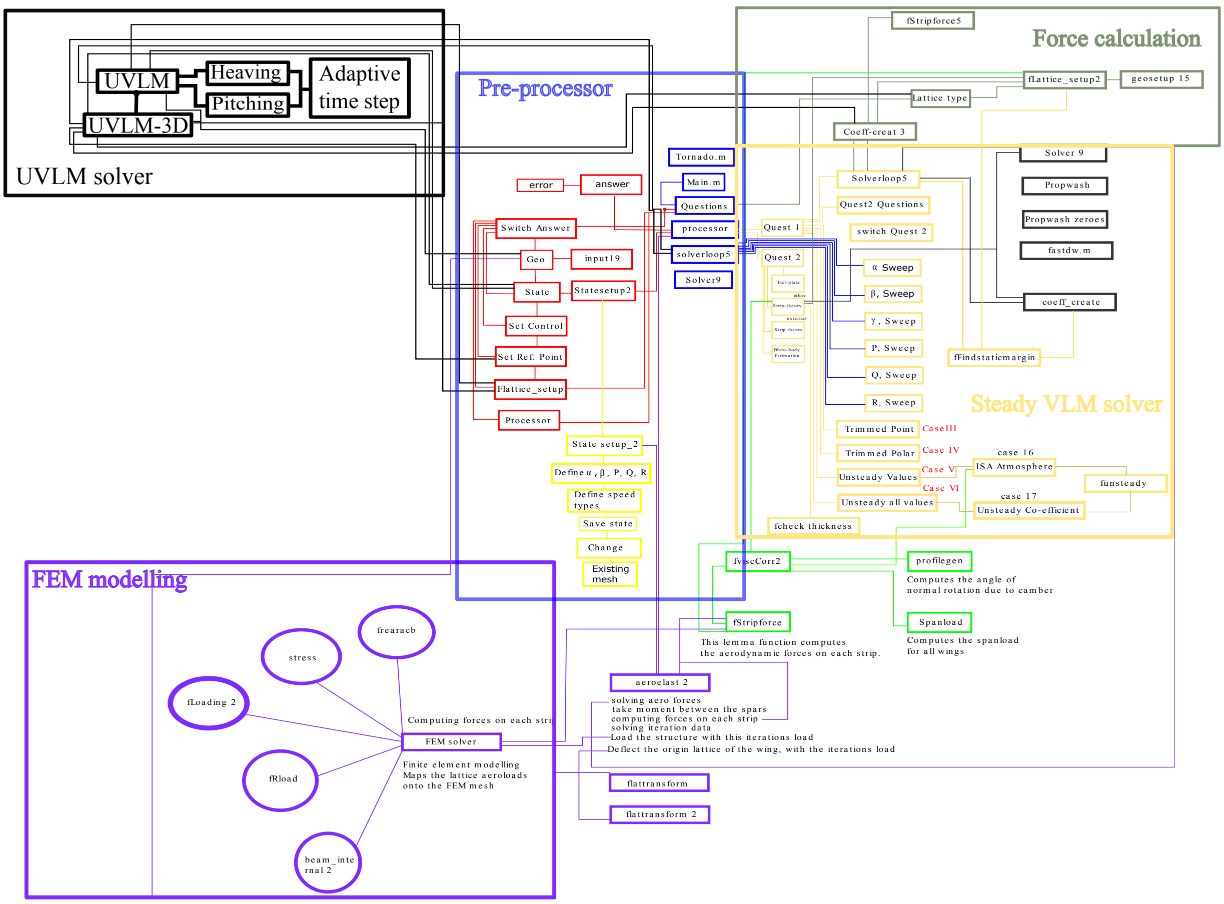

Figure 6: Implementation of UVLM subroutine into Tornado

DOI: 10.13009/EUCASS2023-092

then used in the force coefficients generating subroutine of Tornado to calculate force coefficients and plot the data. UVLM-3D subroutines account for the use of the generated lattice structure from the Tornado base code highlighted in red as shown in Fig. 6 and define its change in orientation or position with time for defined unsteady motion as the function of time and frequency. The shed vortices positions are calculated and redefined to change at every time step which is termed as an influence on the geometry in motion which changes in velocity potentials. This addition to free stream velocity helps in predicting the aerodynamic characteristics of a wing in three-dimensional flow conditions.

The introduction of this solver with a LOM approach gives the potential in solving unsteady aerodynamics of aerofoil under a transient time frame which drastically reduces the design cost of the next generation of aerofoil design. The solver is integrated into the user interface of Tornado to provide the user with a way to define and alter any changes required before executing it. The two fundamental parameters which drive this solver such as uniform flow speed, time step, angle of attack, frequency and amplitude are user-defined. The work in future is to improve its utilisation with other sections of Tornado such as integrating with the steady solver to provide a comparative relation between steady and unsteady motion of an aerofoil under similar conditions, accounting for changes in force coefficients and extracting data for its application into design optimisation.

The advancement of UVLM into the three-dimensional solver, the angle of attack position with body references axis is redefined for every time-step as:

$$\alpha_x = 0.75 \times C \times \cos\alpha \times sx \tag{12}$$

where α_x is the position of the angle of attack in the x direction, C is the chord length, and sx is the change in position of the wing in the x direction with each time-step. Similarly, the α_y is defined as :

$$\alpha_y = 0.75 \times C \times \sin\alpha \times sy \tag{13}$$

where α_y is the position of the angle of attack in the y direction, sy is the change in position of the wing in the y direction with each time step. For pre-processor initialisation location of the lattice is obtained from the lattice setup code of Tornado which helps as initially places a lattice predefined with a defined as the number of lattices on both sides of the aircraft through its wingspan. To define the wake of this aircraft the farstream coordinates are defined which are the function of cosine and sine of the defined angle of attack.

$$infx = infdist \times \cos(\alpha) \times \cos(\beta) \tag{14}$$
$$infy = -infdist \times \sin(\beta) \tag{15}$$
$$infz = infdist \times \sin(\alpha) \times \cos(\beta) \tag{16}$$

In the above equations, $infdist$ is the variable defined for infinite distance based on the reference position of the geometry defined in the geometry setup of Tornado. β is the defined side slip for current flight state. The position of these lattices changes with every time step with defined amplitude and frequency of the motion which is defined as:

$$x = infx + lattice.XYZ(t, c(s), 1) \tag{17}$$
$$y = infy + lattice.XYZ(t, c(s), 2) \tag{18}$$
$$z = infz + lattice.XYZ(t, c(s), 3) \tag{19}$$

In the above equations, s is the variable defined in the lattice setup code file of Tornado which helps in defining which wing of the geometry currently working with. With the use of $infx$ and x lattice position terms with dx as the distance between the wake elements and the initial element position can derive the wake coordinates for each panel in the lattice as:

$$INF1(i, 1, 1) = lattice.XYZ(i, 1, 1) + infx + dx(i, 1) \tag{20}$$

The above equation $INF1$ is defined as the wake initialising coordinate which is the addition of $lattice.XYZ$ x coordinate, $infx$ and dx which are the function flight state conditions. This set of equations runs for the number of S wings symmetrical or non-symmetrical which is defined by the user. Similarly, the equation for y and z coordinates for the wake initialisation is derived as:

$$INF1(i, 1, 2) = lattice.XYZ(i, 1, 2) + infy + dy(i, 1) \tag{21}$$
$$INF1(i, 1, 3) = lattice.XYZ(i, 1, 3) + infz + dz(i, 1) \tag{22}$$

Now to determine the influence of the wake element of interest, the distance between the wake element and the wake element of interest is calculated as is for the 2-D UVLM code;

$$rx = lattice.XYZ(a, i, 1) - lattice.XYZ(1 : a, 1 : it, 1) \tag{23}$$

DOI: 10.13009/EUCASS2023-092

This difference in wake elements helps in identifying the distance of the wake from the initial position of the geometry and how it influences the change of velocity potential for each time step. Similarly, the difference in y and z directions are also derived as:

$$ry = lattice.XYZ(a, i, 2) - lattice.XYZ(1 : a, 1 : it, 2) \tag{24}$$

$$rz = lattice.XYZ(a, i, 3) - lattice.XYZ(1 : a, 1 : it, 3) \tag{25}$$

The parameters rx, ry, rz are used to calculate the change in velocity potential in each direction giving velocities u, v and w. This is then used to move the panel location with reference to local velocity with increasing time-step as:

$$lattice.XYZ(1 : a, 1 : it, 1) = lattice.XYZ(1 : a, 1 : it, 1) + u(1 : it) \times dt \tag{26}$$

$$lattice.XYZ(1 : a, 1 : it, 2) = lattice.XYZ(1 : a, 1 : it, 2) \tag{27}$$

$$lattice.XYZ(1 : a, 1 : it, 3) = lattice.XYZ(1 : a, 1 : it, 3) + v(1 : it) \times dt \tag{28}$$

This helps in plotting the implicit wake of an oscillating wing which is defined by the oscillatory frequency and the amplitude of the motion. This change in motion can be defined by the use of the time-dependent motion or the frequency-dependent motion. The layout for supersonic configuration is shown in Fig. 7 which defines the distribution of the above equations in different sections of the pre-processor, the solver and the post-processor. The addition of an adaptive time-step is not added into this arrangement as it increases the computational time for the supersonic simulations.

4. Results and discussion

The validation of the solver is done by comparing it with experimental[15] and numerical data[1] from early research in unsteady lift predictions. The results are compared for modelled 2-D profile at the Mach number of 0.5 and 0.8 with the profile divided among 100 panels chordwise. The variation of the two-dimensional indicial lift coefficient per angle of attack with chord length travelled is compared with the same boundary conditions as that of the literature.

Compared results as shown in the Fig. 8 show the non-steady region at $Ut/c < 1.3$ which is close to experimental model ($Ut/c < 1$). The plot shows the compared values of C_{L_α} in the units of per radian to that of the chord length travelled in meters. The change into a steady region starts after $Ut/c > 1.4$. Compared results of Change in C_{L_α} with travelled chord length shows a percentage in the error of 26% compared to that of Lomax[15] . The C_{L_α} predictions of higher Ut/c have a higher percentage of error when compared with an experimental and numerical model. The expected results deviate from the experimental model because of the following reasons; one is that by increasing chord length, the accuracy of VLM diminishes. This problem can be rectified by using more panels, increasing the influence terms hence increasing the accuracy. Another reason is the solver's incapability of accurately predicting the correction of the compressibility of the flow. This can be implemented by either using Prandtl Glauret's compressibility correction

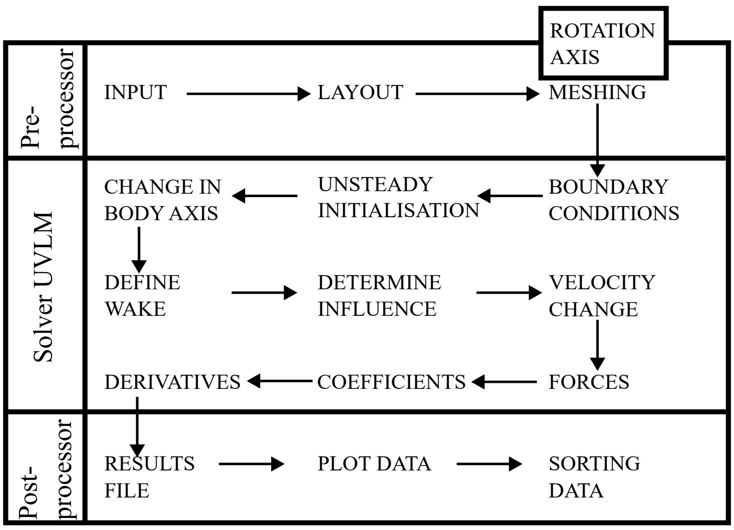

Figure 7: Supersonic 3-D UVLM subroutines in Tornado

DOI: 10.13009/EUCASS2023-092

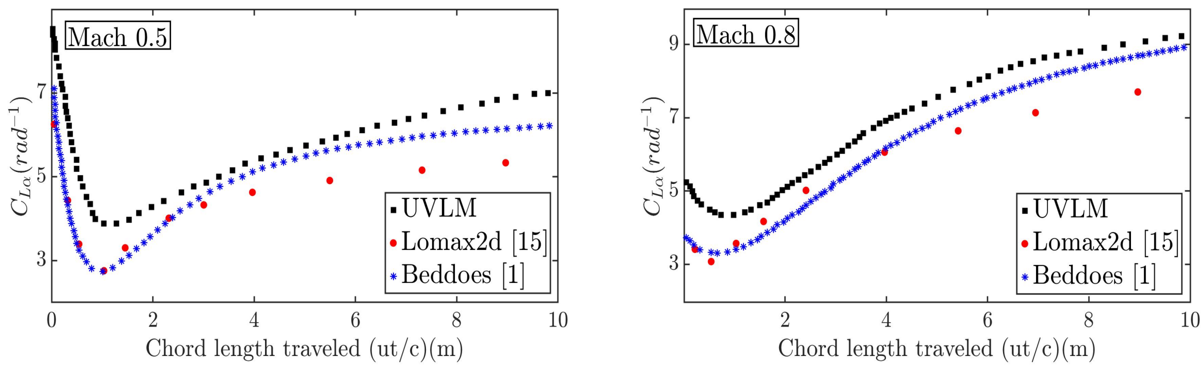

Figure 8: Comparison of change in lift coefficient with alpha in chord length travelled from UVLM 2D and literature,[15].[1]

factor, which only accounts for the subsonic or by using the hybrid approach with conventional CFD as a plugin to start with simulation based on initial results from the UVLM solver for faster convergence. The results from UVLM for two-dimensional analysis using NACA-0012 aerofoil are compared with the literature. The simulation was run for the oscillatory frequency of 4Hz and 1Hz of motions. Defining the motion of an aerofoil is a combination of pitching and heaving as a function of frequency and time-step. The results plots are the comparison between the C_L with increasing time (sec.). Comparison between results obtained from the UVLM code and CFD simulation[9] is shown in Fig.9-12. The results obtained from the code show good agreement with those from[9] . There is a slight shift in the graph which is because of the time-step error, which is not mentioned in the literature. The graph shows accuracy in predicting the force coefficients for the same initial conditions for low-frequency motion. The drag in UVLM is calculated using wake-induced downwash, which is derived from the influence of all the wake elements in a motion. Downwash and rate of change of bound circulation from the shed and bound vortices are used to calculate the drag force, which is the induced drag generated over an aerofoil. In CFD[9] , the drag force is calculated by dividing the force on the aerofoil in the opposite direction to the flow, which is obtained by solving the URANS equations and dividing them by the cross-sectional area of the aerofoil. From the results, it is apparent that the UVLM predictions are reasonably similar when compared with the higher-order CFD simulation results, with a level of accuracy suitable for the preliminary analysis of unsteady effects of aerofoil motion.

The three-dimensional progress with UVLM is achieved by recalculating the new datum point to change the orientation of the panels with respect to the defined angle of attack by the user. Lattice was imported from the Tornado lattice code and is redefined to accommodate the change in no of panel concentration along the wing chord and span. The wake initialisation is done by calculating the infinite distance for x, y and z directions with defined state angles i.e., angle of attack and side angle. Wing panel orientation is redefined with respect to the angle of attack and side-slip angle so the wake reflects that with time. Then the influence of wake elements is defined on adjacent panels and how it reflects with time-step. Then the difference in distance is calculated between all the wake elements and wake elements of interest which were later used to calculate the velocity potential for all directions. The change in wake has been

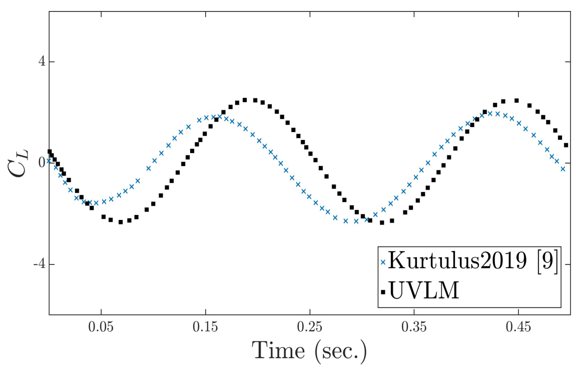

Figure 9: C_L from UVLM code and literature[9] at 4Hz

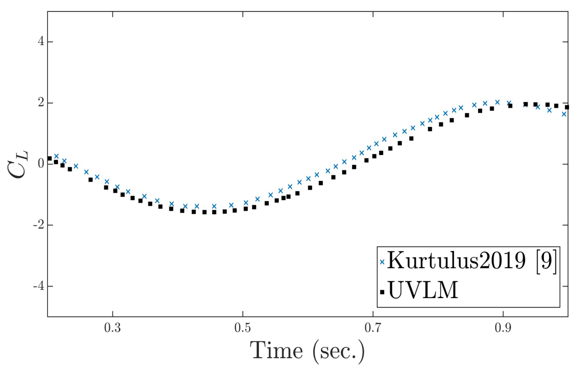

Figure 10: C_L from UVLM code and literature[9] at 1Hz

DOI: 10.13009/EUCASS2023-092

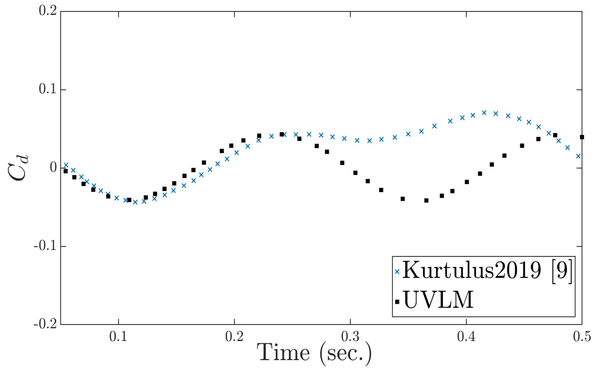

Figure 11: C_d from UVLM code and literature[9] at 4Hz

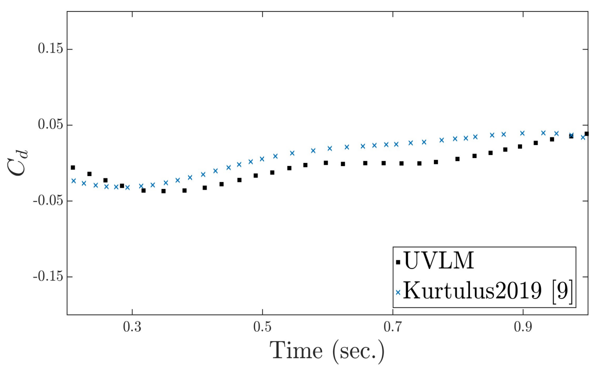

Figure 12: C_d from UVLM code and literature[9] at 1Hz

achieved by moving the wake elements with local velocity. The plot for which is shown in Fig. 13.

With an extension of the three-dimensional build of the unsteady solver, the lattice code derived from the Tornado base code is modified and improved to account for the change in angle of attack with time, also enabling the user to change the dihedral angle and wing orientation and configuration. Further work can be done on improving the viscous correction for this solver and plotting the shed wake and induced wake for each time step which will improve its capabilities to mimic real-world environments. For the buildup of viscous correction term for UVLM, initial terms are defined and are derived from previous code such as the 'N' number of panels chord-wise, and panel information such as location and Reynolds number. Reference viscosity is calculated using the reference chord length from the mean of chord length from all the panels. Then the viscous correction term is calculated using the skin friction term, reference viscosity for a given Mach and Reynolds number for a given panel.

The curves in Fig.14 are shown for sinking and pitching three-dimensional triangular wings for Mach 1.2 and 2 speeds. Besides the similarities in the nature of the curve and solutions, several conclusions can be drawn from these results. Firstly, notice how for shorter chord lengths the value of lift curve slope is always higher for UVLM because of working with the solution of fewer influence terms affecting the convergence. Secondly, with increased chord length the solutions are close to that of the experimental results from the literature[15] giving the same conclusive statement as for the experimental work that since all the characteristics of the triangular wing are independent of the angle of sweep

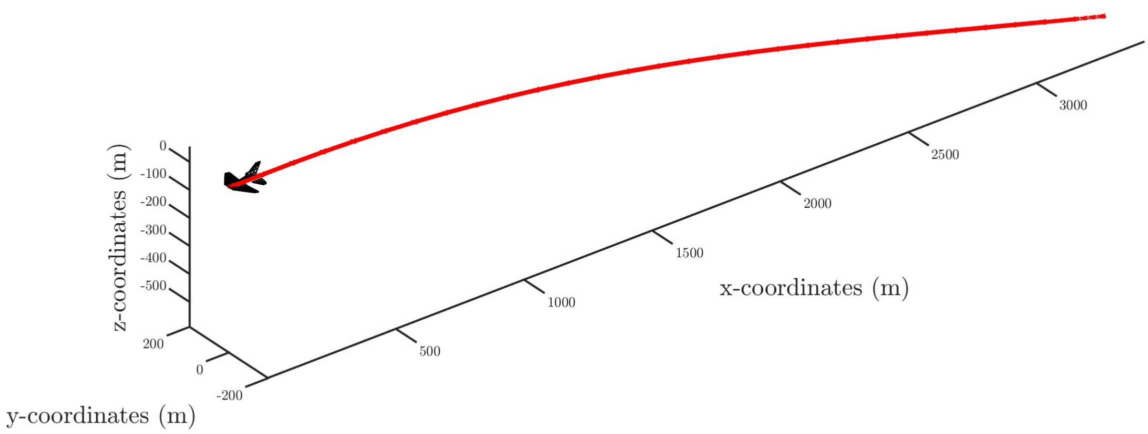

Figure 13: Unsteady wake of F-16 wing.

DOI: 10.13009/EUCASS2023-092

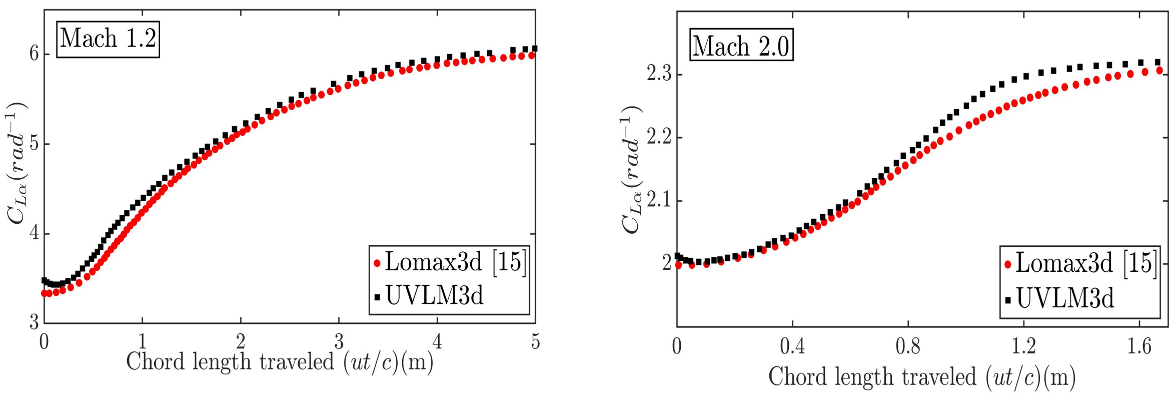

Figure 14: Comparison of change in lift coefficient with alpha in chord length travelled from literature.[15]

for this situation, the results can be said to be valid for the un-yawed triangular wing as long as the edges are supersonic. This means that, as the VLM does not account for the thickness of the wings, and therefore edges designed through VLM are assumed to be supersonic, the validity of the solver can be found effective for any supersonic configuration of the wing. Thirdly, the initial values of $C_L\alpha$ depend on the influence terms from shed vortices and bound vortices which are directly dependent on chord length travelled and also influenced by the Mach number. With increased Mach number the positions of the shed vortices calculated are not accurate, which affects its influence on the results and as seen from Fig. 14 the accuracy of the solver deviates with increasing chord length travelled. It is observed that the results for three-dimensional profiles match better with the experimental data of Lomax3-d[15] when compared with the 2-D UVLM solver because in the development of the three-dimensional solver, the initial Tornado code is used to define the panel geometry, initialising the boundary condition and which undergoes the application of Prandtl Glauret's compressibility correction factor which is not used for the two-dimensional solver. The accuracy of the solver can be increased by increasing the number of panels chordwise and spanwise. Having a larger grid of panels provides more data with a change in velocity potential. The implementation of the Mach-cone influence[6,8] is also suggested for better prediction of the panel collocation points. This will help in identifying the location shift when transitioning from subsonic to supersonic speeds.

5. Conclusion

The proposed work highlights the similarities and differences between the two-dimensional and the three-dimensional solver in terms of accuracy and agreement with experimental data and the high-fidelity CFD solver. It discusses the factors influencing lift curve slope and the potential for improving solver accuracy through increased panel density and Mach-cone influence. The two-dimensional UVLM solver compared to experimental and numerical models shows a non-steady region at $Ut/c < 1.3$, which is close to the experimental model ($Ut/c < 1$). The transition into a steady region begins after $Ut/c > 1.4$. The overall curve matches that of experiments and literature. However, predictions of $C_{L\alpha}$ at higher Ut/c values have a higher percentage of error mainly due to the UVLM's lack of correction for compressibility effects in two-dimensional flow.

The three-dimensional solver shows better agreement with experimental data compared to the two-dimensional UVLM solver. The three-dimensional solver uses Tornado's defined panel geometry, initializes boundary conditions, and applies Prandtl-Glauert's compressibility correction factor. These additional factors enhance the accuracy of the solver compared to the two-dimensional solver. The accuracy of the solver can be improved by increasing the number of panels chordwise and spanwise, resulting in a larger panel grid and more data for velocity potential changes. Additionally, implementing the Mach-cone influence is suggested for better prediction of panel collocation points and identifying location shifts during the transition from subsonic to supersonic speeds.

DOI: 10.13009/EUCASS2023-092

References

[1] T.S. Beddoes. Practical computation of unsteady lift. . Technical report, Vertica, 1984.

[2] S M Belotserkovskii. Study of the Unsteady Aerodynamics of Lifting Surfaces Using the Computer. *Annual Review of Fluid Mechanics*, 9(1):469–494, 1977.

[3] Enrique Mata Bueso, A. Rizzi, and J. Oppelstrup. *Unsteady Aerodynamic Vortex Lattice of Moving Aircraft, Master thesis*. PhD thesis, KTH, 2011.

[4] D G Crighton. The Kutta Condition in Unsteady Flow. *Annual Review of Fluid Mechanics*, 17(1):411–445, 1 1985.

[5] Earl Dowell, Kenneth Hall, Jeffrey Thomas, Razvan Florea, Bogdan Epureanu, and Jennifer Heeg. Reduced order models in unsteady aerodynamics. In *40th Structures, Structural Dynamics, and Materials Conference and Exhibit*, volume 1, pages 622–637, Reston, Virigina, 4 1999. American Institute of Aeronautics and Astronautics.

[6] Ester Garrido Estrada, Tomas Melin, and Ester Garrido Estrada. *Tornado supersonic module development (Master's thesis)*. Linköping University, 2010.

[7] M. E. Goldstein and H. Atassi. A complete second-order theory for the unsteady flow about an airfoil due to a periodic gust. *Journal of Fluid Mechanics*, 74(4):741–765, 4 1976.

[8] Daniel Guillermo-Monedero, Clifford A Whitfield, Richard J Freuler, and Matthew H Mccrink. *A Comparison of Euler Finite Volume and Supersonic Vortex Lattice Methods used during the Conceptual Design Phase of Supersonic Delta Wings (Master's thesis)*. Ohio State University, Columbus, U.S.A, 2020.

[9] Dilek Funda Kurtulus. Unsteady aerodynamics of a pitching NACA 0012 airfoil at low Reynolds number. *International Journal of Micro Air Vehicles*, 11:175682931989060, 1 2019.

[10] H.G. Kussner. Zusammenfassender Bericht über den instationären Auftrieb von Flügeln. Technical Report 12, Luftfahrt-Forschung, 1936.

[11] Daniel Levin and Joseph Katz. Vortex-Lattice Method for the Calculation of the Nonsteady Separated Flow over Delta Wings. *Journal of Aircraft*, 18(12):1032–1037, 1981.

[12] Kai Li, Jiaqing Kou, and Weiwei Zhang. Unsteady aerodynamic reduced-order modeling based on machine learning across multiple airfoils. *Aerospace Science and Technology*, 119:107173, 12 2021.

[13] Zhenyao LI, Lihao FENG, and Jinjun WANG. Individual influence of pitching and plunging motions on flow structures over an airfoil during dynamic stall. *Chinese Journal of Aeronautics*, 33(3):840–851, 3 2020.

[14] Minxiao Lin, Shijun Guo, Shun He, Wenhao Li, and Daqing Yang. Structure health monitoring of a composite wing based on flight load and strain data using deep learning method. *Composite Structures*, 286:115305, 4 2022.

[15] Harvard Lomax, Max A Heaslet, Franklyn B Fuller, and Loma Sluder. Two-and three-dimensional unsteady lift problems in high-speed flight. Technical Report 1, NASA Langley Research Center, NACA-TR-1077, 1952.

[16] Tomas Melin. *User's guide and reference manual for Tornado.* Royal Institute of Technology, 2000.

[17] Luis R Miranda, Robert D Elliott, and William M Baker. A Generalized Vortex Lattice Method for Subsonic and Supersonic Flow Applications. Technical report, NASA-CR-2865, NASA Langley Research Center, 1977.

[18] M. Moriche, O. Flores, and M. García-Villalba. On the aerodynamic forces on heaving and pitching airfoils at low Reynolds number. *Journal of Fluid Mechanics*, 828:395–423, 10 2017.

[19] E Pistolesi. Ground Effect - Theory and Practice. Technical report, NACA-TM-828, National Advisory Committee of Aeronautics, 1937.

[20] Daniella E. Raveh. Reduced-Order Models for Nonlinear Unsteady Aerodynamics. *AIAA Journal*, 39(8):1417–1429, 8 2001.

[21] C. Rehbach. Numerical calculation of three-dimensional unsteady flows with vortex sheets. In *16th Aerospace sciences meeting*, Huntsville, AL, U.S.A., 16-18 January, 1978. American Institute of Aeronautics and Astronautics (AIAA).

DOI: 10.13009/EUCASS2023-092

[22] P. D. Sclavounos. An unsteady lifting-line theory. *Journal of Engineering Mathematics*, 21(3):201–226, 1987.

[23] Luke R. Smith and Anya R. Jones. Vortex formation on a pitching aerofoil at high surging amplitudes. *Journal of Fluid Mechanics*, 905:A22, 12 2020.

[24] Paulo A. O. Soviero and Fabiano Hernandes. Compressible Unsteady Vortex Lattice Method for Arbitrary Two-Dimensional Motion of Thin Profiles. *Journal of Aircraft*, 44(5):1494–1498, 9 2007.

[25] Haithem E. Taha and Amir S. Rezaei. On the high-frequency response of unsteady lift and circulation: A dynamical systems perspective. *Journal of Fluids and Structures*, 93:102868, 2 2020.

[26] Theodore Theodorsen. General theory of aerodynamic instability and the mechanism of flutter. Technical report, National Advisory Committee of Aeronautics, 1949.

[27] Siddhartha Verma, Guido Novati, Flavio Noca, and Petros Koumoutsakos. Fast Motion of Heaving Airfoils. *Procedia Computer Science*, 108:235–244, 1 2017.

[28] Herbert Wagner. Über die Entstehung des dynamischen Auftriebes von Tragflügeln. *ZAMM - Zeitschrift für Angewandte Mathematik und Mechanik*, 5(1):17–35, 1925.

[29] You Wu, Yuting Dai, Chao Yang, and Guangjing Huang. Unsteady and nonlinear aerodynamic prediction of airfoil undergoing large-amplitude pitching oscillation based on gated recurrent unit network. *Proceedings of the Institution of Mechanical Engineers, Part G: Journal of Aerospace Engineering*, 237(2):270–284, 2 2023.

[30] X. Xia and K. Mohseni. Unsteady aerodynamics and vortex-sheet formation of a two-dimensional airfoil. *Journal of Fluid Mechanics*, 830:439–478, 11 2017.

[31] Li Xiaohua, Zheng Guo, Grecov Dana, and Zhongxi Hou. Efficient reduced-order modeling of unsteady aerodynamics under light dynamic stall conditions. *Proceedings of the Institution of Mechanical Engineers, Part G: Journal of Aerospace Engineering*, 233(6):2141–2151, 5 2019.